SUPPORTING INFORMATION

Interface Control of PEC Water Oxidation Performance with $Ni_{1-x}Fe_xO_y$ Modified Hematite Photoanodes

Hamed Hajibabaei, Abraham R. Schon, Thomas W. Hamann*

Department of Chemistry, Michigan State University, East Lansing, Michigan 48824-1322,

United States

Table S1. The weight of metal precursor used to prepare the catalyst solutions.

Composition	Fe (mg)	Ni (mg)	Hexane (mg)
NiO_y	0	20	90
$Ni_{0.75}Fe_{0.25}O_y$	103	141	920
$Ni_{0.5}Fe_{0.5}O_y$	44	20	212
$Ni_{0.25}Fe_{0.75}O_y$	411	63	1440
FeO_y	50	0	142

Table S2. a) Composition of as prepared $Ni_{1-x}Fe_xO_y$ catalysts found by XPS, the compositions and the error bars are the average and standard deviations acquired from 3 independently prepared samples, respectively, b) comparison between catalyst composition before and after electrochemical conditioning on the same electrode. * Samples were conditioned by cycling the potential at 1.0 – 2.0 V *vs.* RHE for 40 cycles as well as electrochemical characterization by impedance at potential range of 1.3-1.8 V *vs.* RHE with 100 mV interval. Afterwards the electrodes were rinsed with extensive amount of DI water.

a)

	As prepared			
	Theoretical		Found	
Composition	% Ni	% Fe	% Ni	% Fe
NiO_y	100	0	100	0
$Ni_{0.75}Fe_{0.25}O_y$	75	25	73 ± 6	27 ± 6
$Ni_{0.5}Fe_{0.5}O_y$	50	50	55 ± 4	45 ± 4
$Ni_{0.25}Fe_{0.75}O_y$	25	75	28 ± 5	72 ± 5
FeO_y	0	100	0	100

b)

	As prepared				*After Conditioning	
	Theoretical		Found			
Composition	% Ni	% Fe	% Ni	% Fe	% Ni	% Fe
NiO_y	100	0	100	0	80	20
$Ni_{0.75}Fe_{0.25}O_y$	75	25	71	29	70	30
$Ni_{0.5}Fe_{0.5}O_y$	50	50	52	48	49	51
$Ni_{0.25}Fe_{0.75}O_y$	25	75	28	72	29	71
FeO_y	0	100	0	100	0	100

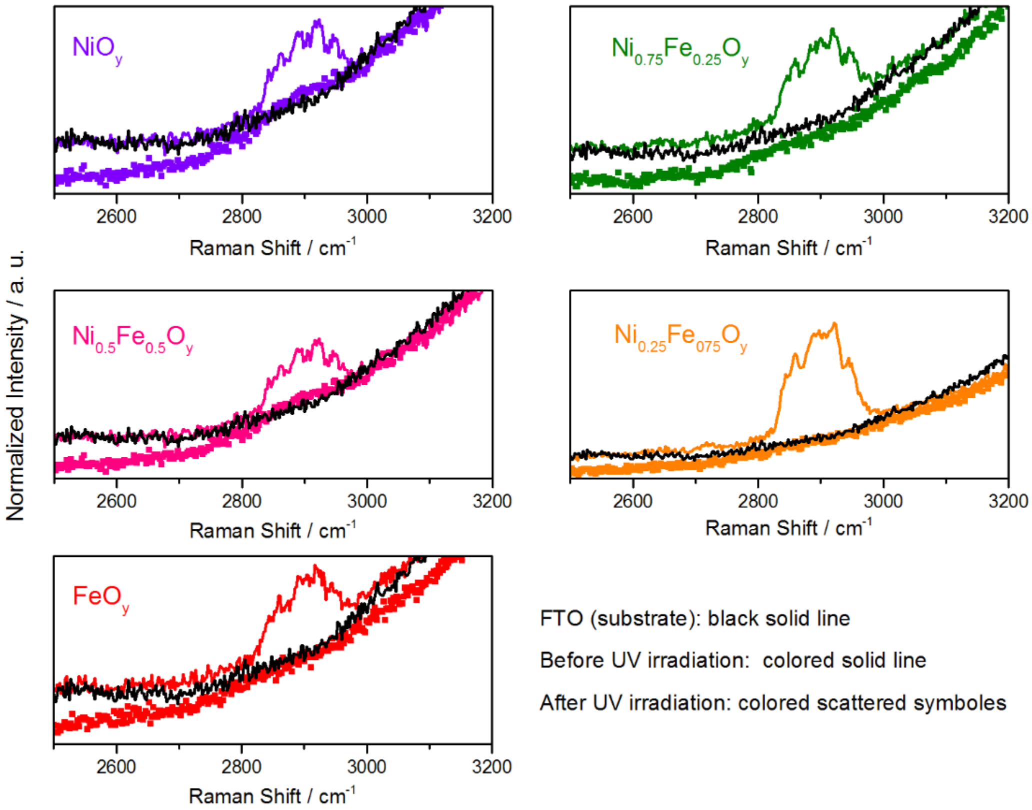

Figure S1. Raman spectra of thin films of $Ni_{1-x}Fe_xO_y$ with different composition before and after irradiation with *UV*-light for 1h. The loss of the bands after *UV*-irradiation indicates that ligands are decomposed.

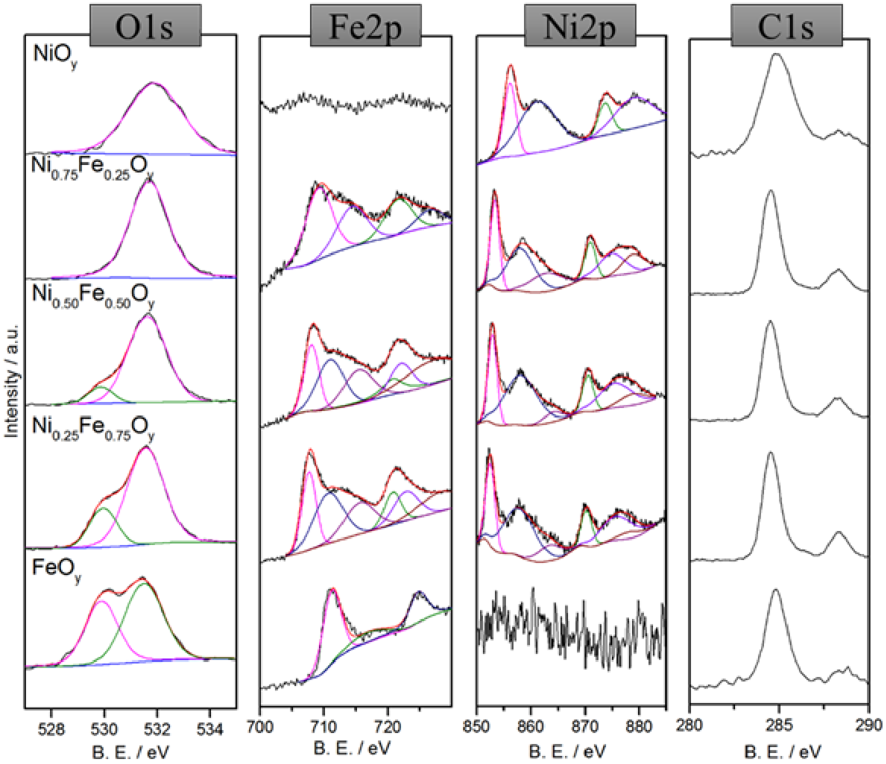

Figure S2. The detailed XPS spectrum of the $Ni_{1-x}Fe_xO_y$ catalyst on FTO. Note: The C1s peaks are presented to show that the shift caused by charging the sample during the measurement are correctly accounted for.

The O 1s, Fe 2p, Ni 2p, and C 1s peaks as a function of composition of the catalyst are shown in Figure S1. The main features of the XPS data are better captured by plotting the peak of each element as a function of the composition of the catalyst. For FeO_y film, two peaks in O1s region (530 and 531.7 eV) and one group of peaks in Fe2p region (711 and 724 eV) were observed. This is in agreement with the formation of FeOOH phase.[1] For NiO_y, on the other hand, only one O1s peak (531.7 eV) and one group of Ni 2p peaks (850 and 860 eV) were observed which is consistent with formation of $Ni(OH)_2$ phase.[1] Interestingly, upon doping $Ni(OH)_2$ with iron, at the maximum concentration of 25%, the peak position of the Fe 2p and Ni2p were shifted to the lower binding energies and only one O1s peak (~531.7 eV) was observed. However, at concentrations beyond 25%, a new O1s peak emerged which is consistent with the formation of FeOOH. Consistent with the oxygen peak, in Fe2p region, up to 25% of the iron, there is only one group of Fe2p peak. At higher concentration of iron, however, a new group of Fe2p peaks emerged which were located at the same position as the Fe2p peaks for FeOOH. In addition, in the Ni2p region a new group of Ni2p peaks emerged which was independent to the composition of the films. Therefore, the presence of one O1s peak and one group of Fe2p peak for the iron content up to 25% indicates that iron is in fact doped into the nickel phase which formed a single phase of $Ni_{1-x}Fe_xO_y$. On the other hand, at the higher concentration of iron two distinctive phases of FeOOH and $Ni_{1-x}Fe_xO_y$ were formed. This finding is consistent with previous reports on the electrocatalytic activity of $Ni_{1-x}Fe_xO_y$ on different substrates.[1,2]

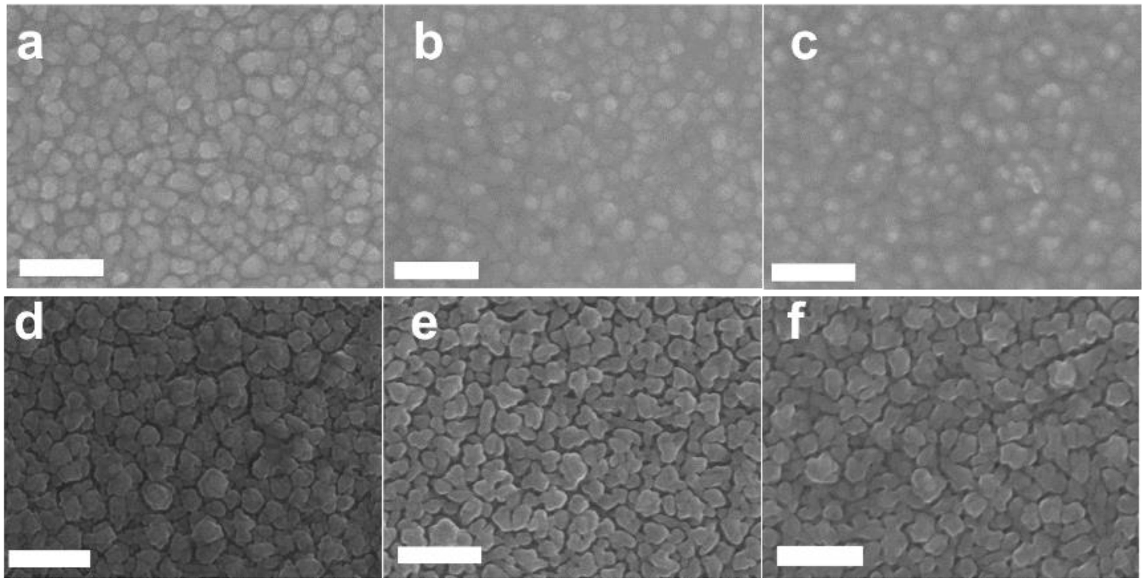

Figure S3. The SEM images of bare and catalyst coated ALD (a-c), ED (d-e) electrodes. The first column represents the bare electrodes, the 2nd and 3rd columns represent the electrodes coated with $Ni_{0.25}Fe_{0.75}O_y$ and $Ni_{0.75}Fe_{0.25}O_y$, respectively. The scale bare is 500 nm with a magnification of 50K.

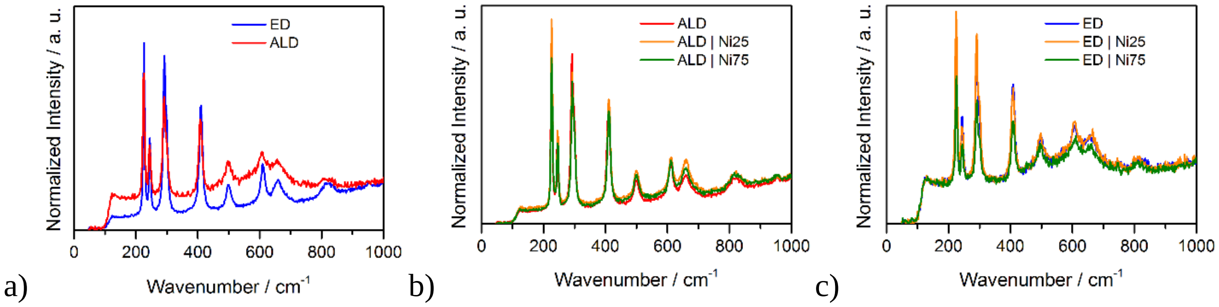

Figure S4. The Raman spectrum of a) bare hematite, b) bare and catalyst modified ALD, c) bare and catalyst modified ED hematite electrodes.

The Raman spectrum of the bare and catalyzed hematite electrodes are shown in Figure S4. All the observed peaks are readily assigned to α-Fe_2O_3. Clearly, the Raman spectrum of hematite films, i.e. ALD and ED, are almost identical which further indicates that regardless of the preparation method the degree of crystallinity and crystal orientations for both type of hematite films are similar. In addition, after coating hematite electrodes with catalysts, the Raman spectrum of the bare and catalyst coated hematite films, in terms of peak position, shape, and patterns, are identical.

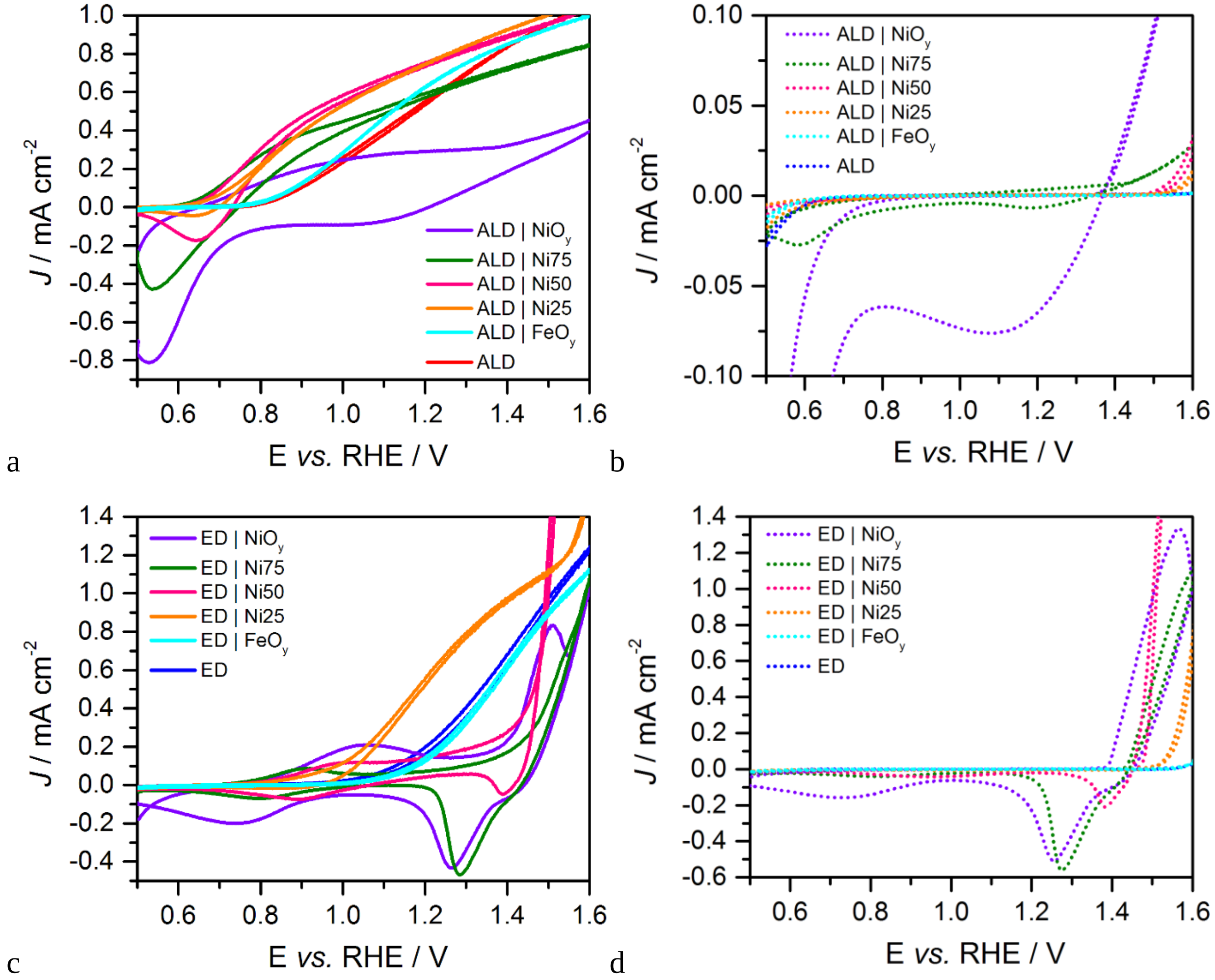

Figure S5. *J-E* curves measured in light (a and c) dark (b and d) for bare and catalyst coated ALD (top), and ED (below) hematite electrodes in contact with 1 M KOH solution. The plots correspond to bare ALD (red), bare ED (blue), NiO_y coated hematite (violet), Ni75 coated hematite (green), Ni50 coated hematite (pink), Ni25 coated hematite (orange), and FeO_y coated hematite (cyan).

Batch-1

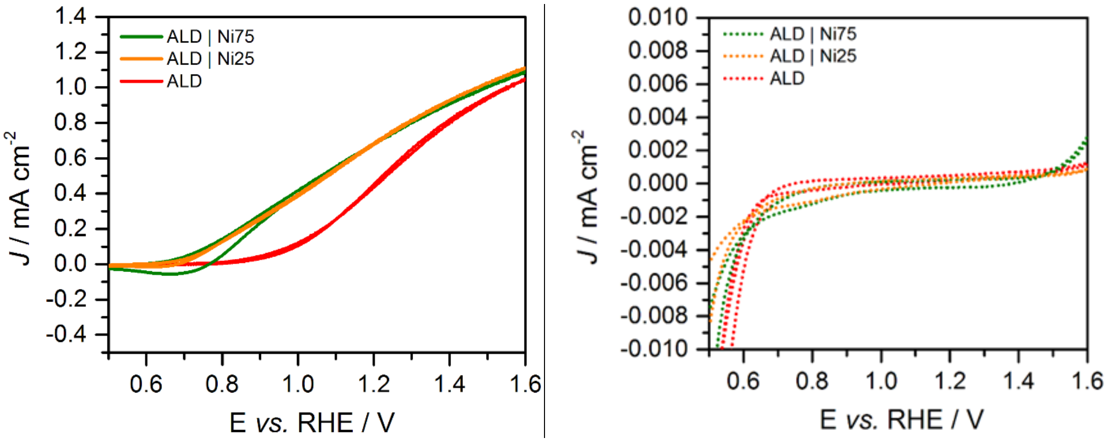

Batch-2

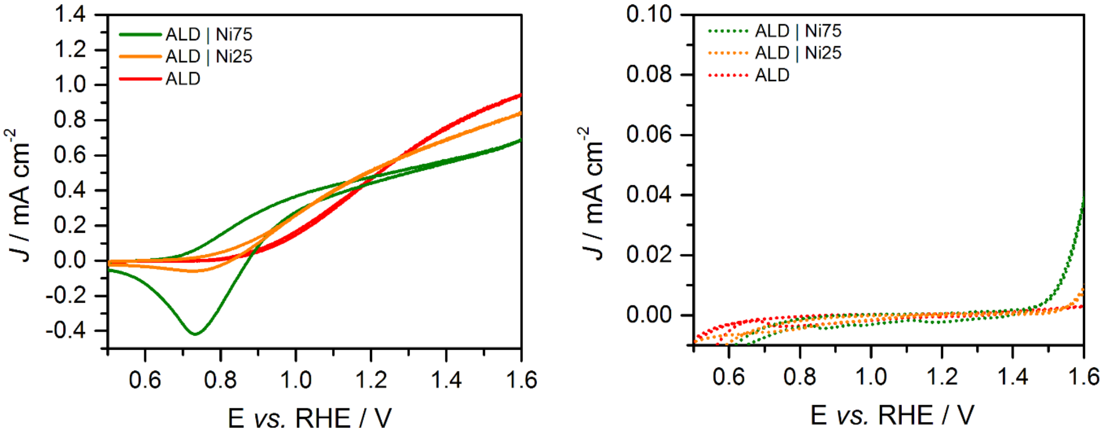

Batch-3

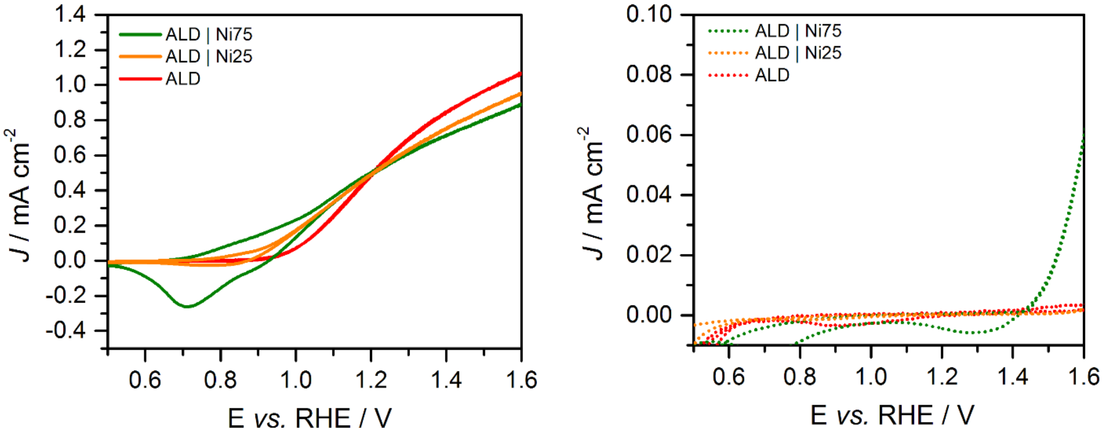

Figure S6. *J-E* curves measured in light (left plots, solid lines) and dark (right plots, dotted lines) for three different batch of ALD hematite electrodes coated with catalyst in contact with 1 M KOH solution; bare ALD (red), Ni75 coated hematite (green), Ni25 coated hematite (orange). Note: these electrodes are different from the one shown in the main text.

Batch-1

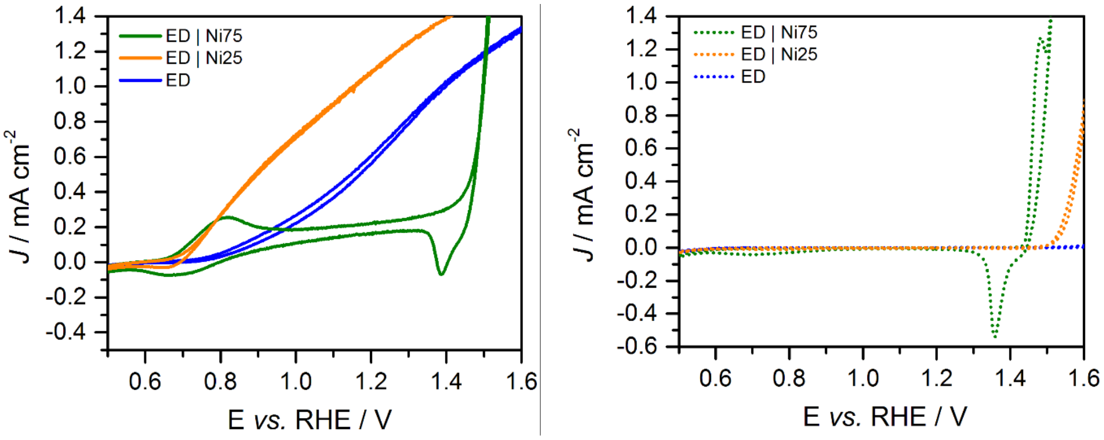

Batch-2

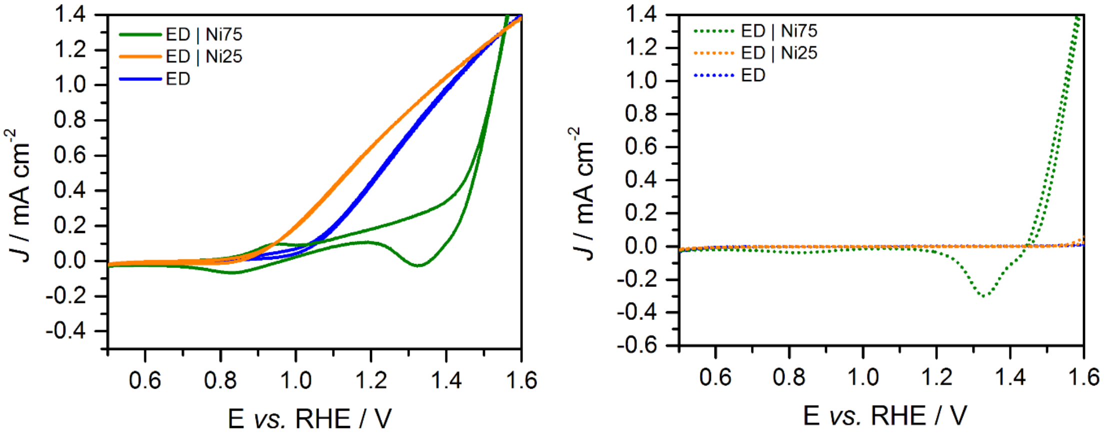

Batch-3

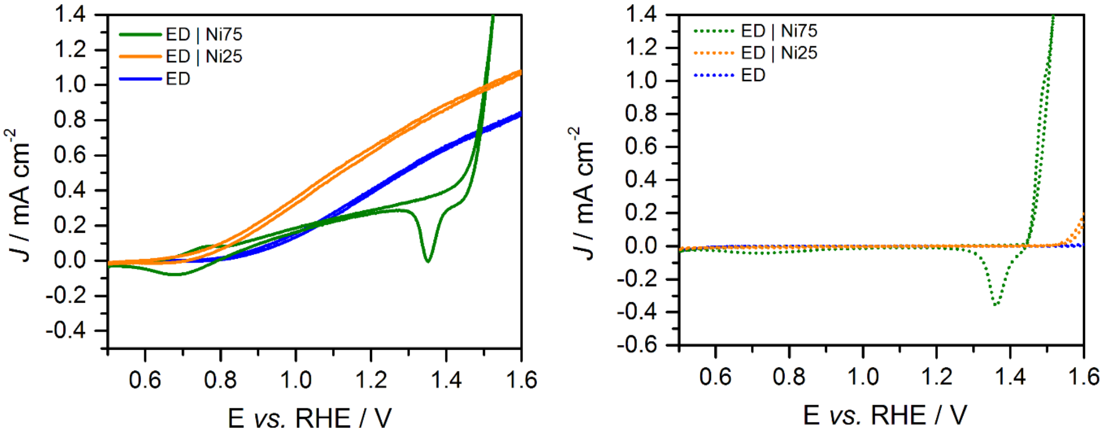

Figure S7. *J-E* curves measured in light (left plots, solid lines) and dark (right plots, dotted lines) for three different batch of ED hematite electrodes coated with catalyst in contact with 1 M KOH solution; bare ED (blue), Ni75 coated hematite (green), Ni25 coated hematite (orange). Note: these electrodes are different from the one shown in the main text

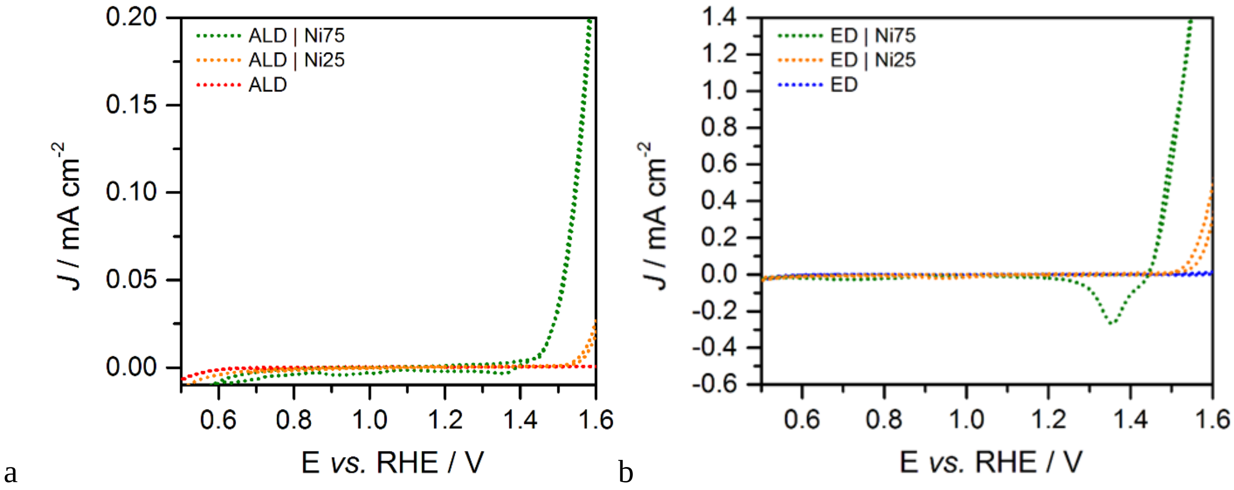

Figure S8. *J-E* curve measured in dark for bare and catalyst coated a) ALD, and b) ED hematite electrodes in contact with 1 M KOH solution.

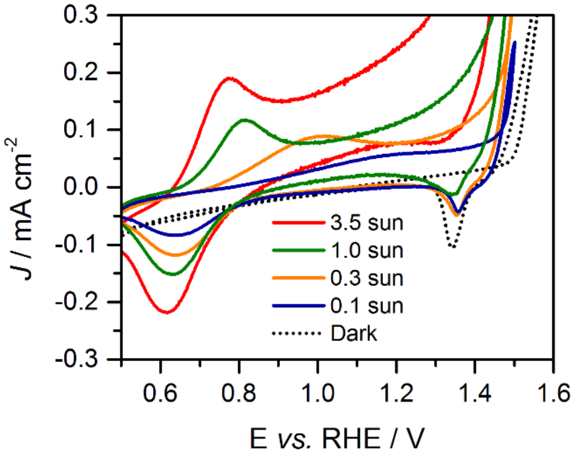

Figure S6. *J-E* curves measured at 20 mV s^{-1} for ED coated electrodes with Ni75 in contact with 1 M KOH solution as a function of illumination intensity.

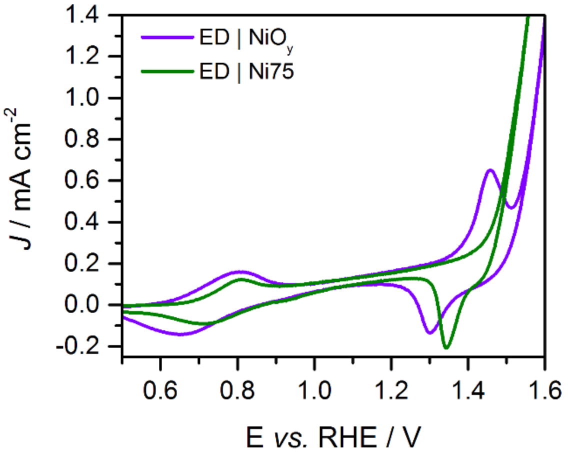

Figure S7. *J-E* curves measured at 20 mV s^{-1} under 1 sun illumination for NiO$_y$ and Ni75 coated ED electrodes in contact with 1 M KOH solution.

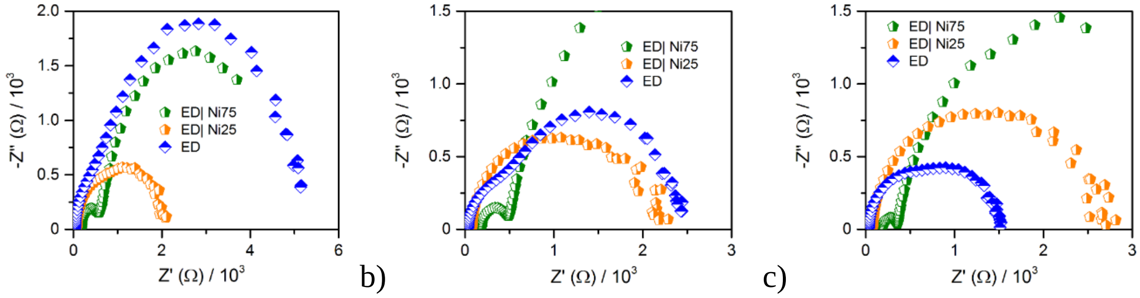

a) b) c)

Figure S8 Nyquist plots for bare and catalyst coated ED electrodes measured under illumination at a) 1.0, b) 1.2, and c) 1.4 V *vs.* RHE.

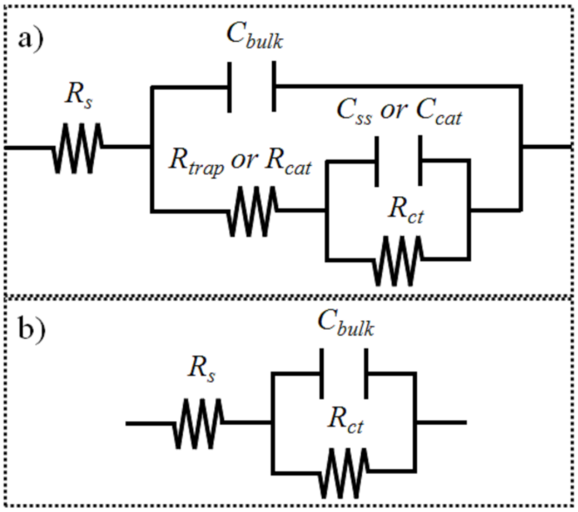

Figure S9 a) Equivalent circuit used for interpretation of bare and catalyst coated ED electrodes, b) Randle circuit when two and one semicircle was observed, respectively.[3]

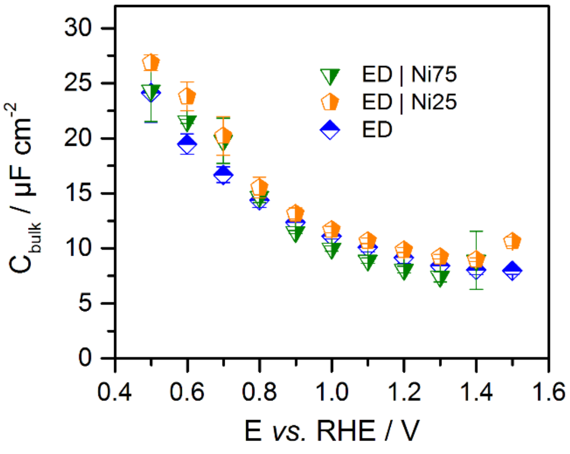

a)

Figure S10. C_{bulk} values fit from EIS measurements for bare and catalyst coated ED electrodes under 1sun illumination in contact with 1M KOH.

Number of cycle	Integrated charge from CV (mC cm^{-2})	Calculated thickness from integrated charge (nm) [a]	Measured thickness with AFM (nm)	Measured thickness with SE (nm)
1	0.8	15.4	17.8	15
2	1.58	30.5	37.4	29
3	2.2	42.4	48.9	42

[a] *For calculation of the thickness the measured composition found by XPS was used and assumed that only Ni atoms are involved in the redox reaction. The cell volume of 0.2108* nm^3 *(ICSD 159700) for Ni-Fe layered double hydroxide and the geometrical surface area were used to calculate the thickness of the film.*[4–6] *For these calculation it was assumed that there is only one Ni per unit cell. Obviously if the number of Ni ion per unit cell is more, the calculated thickness would be smaller. However it does not violate the conclusion that the thickness grows with the number of cycles.*

Table S3. The measured and calculated thickness of the Ni75 on silicon and hematite.

Number of cycle	Measured thickness with AFM (nm)	Measured thickness with SE (nm)
1	13.0	10.0
2	14.0	15.5
3	20.5	23.0

Table S4. The measured thicknesses of the Ni25 on silicon.

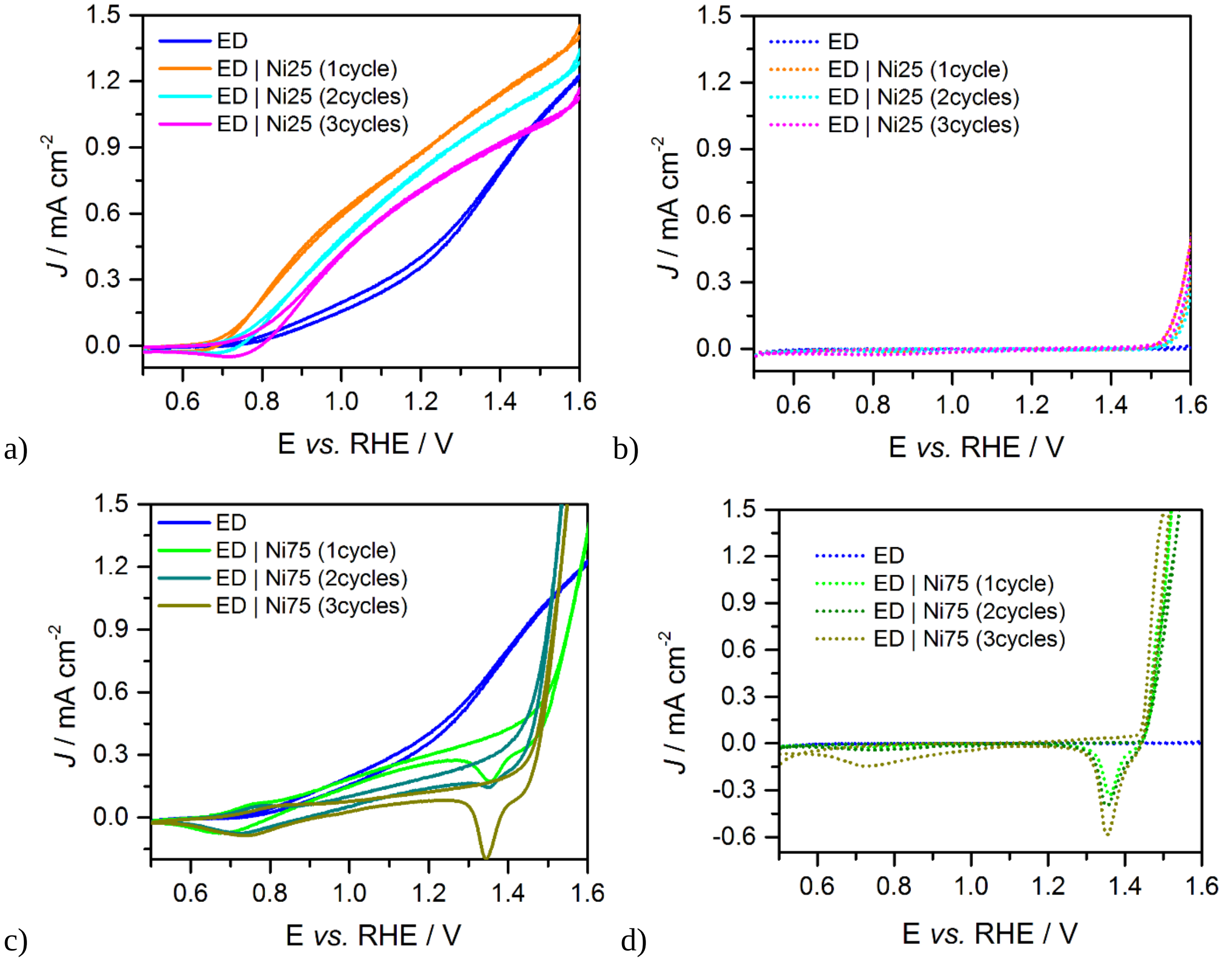

Figure S11. *J-E* curves measured for bare (blue) and Ni25 (a-b) and Ni75 (c-d) coated ED electrodes; a) Ni25 (light), b) Ni25 (dark), c) Ni75 (light), and d) Ni75 (dark) in contact with 1 M KOH solution.

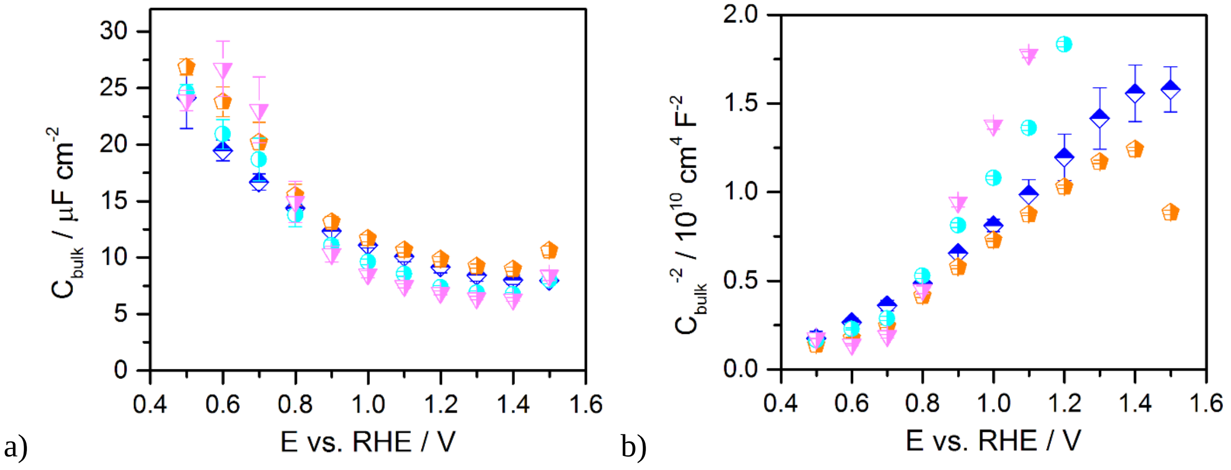

Figure S12. a) C_{bulk}, and b) Mott-Schottky values fit from EIS data for bare and Ni25 coated ED electrodes with 1cycle (pentagon), 2 cycles (circle), and 3 cycles (triangle pointing down). Also included are the value measured for the bare electrode (blue diamond).

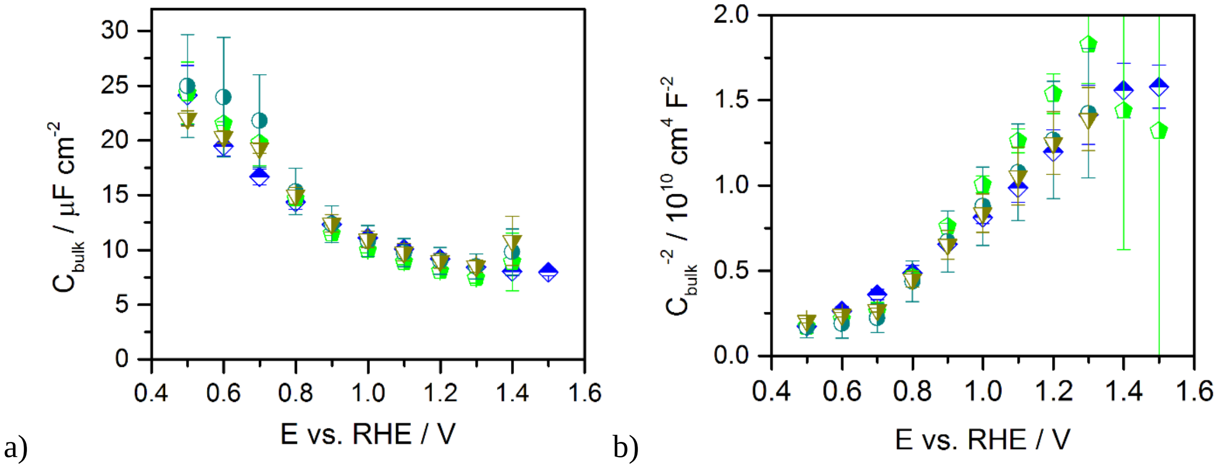

Figure S13. a) C_{bulk}, and b) Mott-Schottky values fit from EIS data for bare and Ni75 coated ED electrodes with 1cycle (pentagon), 2 cycles (circle), and 3 cycles (triangle pointing down). Also included are the value measured for the bare electrode (blue diamond).

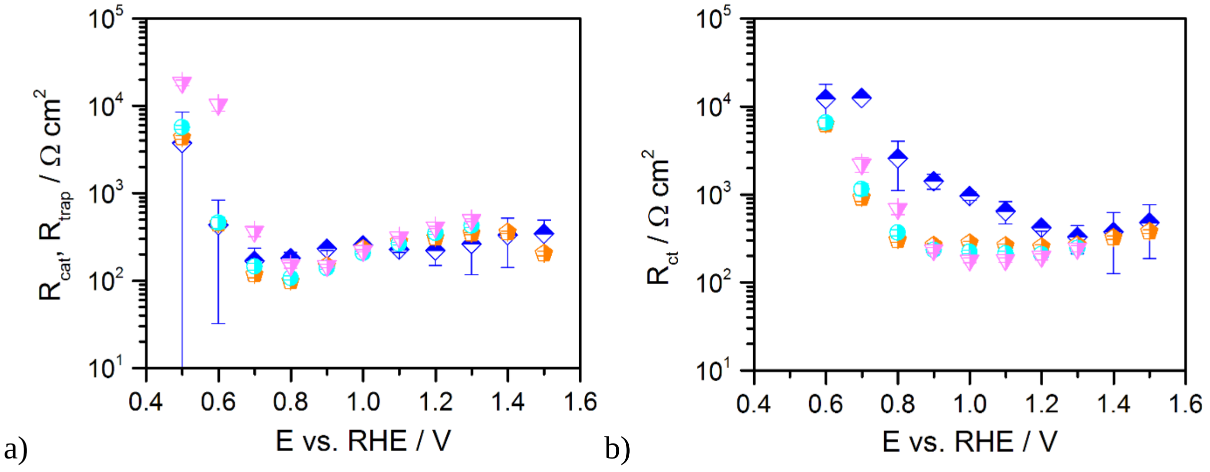

Figure S14. a) $R_{cat,Ni25}$ and b) $R_{ct,Ni25}$ values fit from impedance response of ED hematite electrodes with 1cycle (pentagon), 2 cycles (circle), and 3 cycles (triangle pointing down). Bare ED hematite fitting $R_{trap,bare}$ and $R_{ct,bare}$ (blue diamond) are shown for comparison.

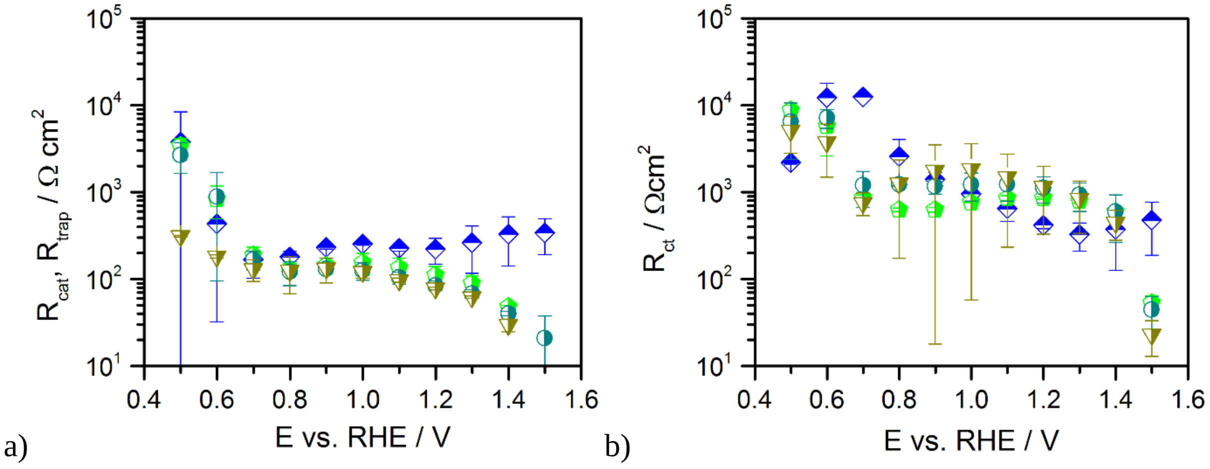

Figure S15. a) $R_{cat,Ni75}$ and b) $R_{ct,Ni75}$ values fit from impedance response of ED hematite electrodes with 1cycle (pentagon), 2 cycles (circle), and 3 cycles (triangle pointing down). Bare ED hematite fitting $R_{trap,bare}$ and $R_{ct,bare}$ (blue diamond) are shown for comparison.

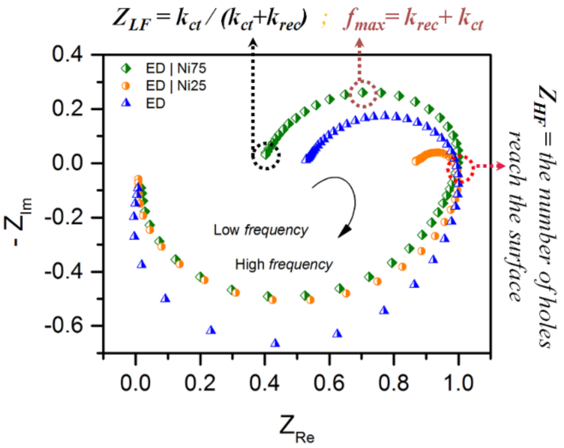

Figure S16. Complex plots of normalized IMPS data for bare and catalyst coated ED electrodes at 1.3 V vs. RHE; bare electrode (blue triangle), Ni75 modified ED electrode (green diamond), and Ni25 coated ED electrode (orange pentagon).

References

(1) Klaus, S.; Louie, M. W.; Trotochaud, L.; Bell, A. T. Role of Catalyst Preparation on the Electrocatalytic Activity of Ni_{1-X} Fe_xOOH for the Oxygen Evolution Reaction. *J. Phys. Chem. C* **2015**, 150719145148001.

(2) Klaus, S.; Cai, Y.; Louie, M. W.; Trotochaud, L.; Bell, A. T. Effects of Fe Electrolyte Impurities on $Ni(OH)_2$/NiOOH Structure and Oxygen Evolution Activity. *J. Phys. Chem. C* **2015**, *119* (13), 7243–7254.

(3) Klahr, B.; Gimenez, S.; Fabregat-Santiago, F.; Bisquert, J.; Hamann, T. W. Photoelectrochemical and Impedance Spectroscopic Investigation of Water Oxidation with "Co–Pi"-Coated Hematite Electrodes. *J. Am. Chem. Soc.* **2012**, *134* (40), 16693–16700.

(4) Nakahira, A.; Kubo, T.; Murase, H. Synthesis of LDH-Type Clay Substituted With Fe and Ni Ion for Arsenic Removal and Its Application to Magnetic Separation. *IEEE Trans. Magn.* **2007**, *43* (6), 2442–2444.

(5) Iwasaki, T.; Yoshii, H.; Nakamura, H.; Watano, S. *Simple and Rapid Synthesis of Ni–Fe Layered Double Hydroxide by a New Mechanochemical Method*; 2012; Vol. 58.

(6) Li, Y.; Li, H.; Yang, M.; He, X.; Ni, P.; Kang, L.; Liu, Z.-H. Topochemical Synthesis of Ni^{2+}–Fe^{3+} Layered Double Hydroxides with Large Size. *Appl. Clay Sci.* **2011**, *52* (1), 51–55.